European Journal of Environmental and Civil Engineering

ISSN: 1964-8189 (Print) 2116-7214 (Online) Journal homepage: https://www.tandfonline.com/loi/tece20

Live load effect in soil-steel flexible culvert: role of apparent cohesion of backfill

Maciej Sobótka & Dariusz Łydżba

To cite this article: Maciej Sobótka & Dariusz Łydżba (2019): Live load effect in soil-steel flexible culvert: role of apparent cohesion of backfill, European Journal of Environmental and Civil Engineering, DOI: 10.1080/19648189.2019.1670264

To link to this article: https://doi.org/10.1080/19648189.2019.1670264

EUROPEAN JOURNAL OF ENVIRONMENTAL AND CIVIL ENGINEERING
https://doi.org/10.1080/19648189.2019.1670264

Live load effect in soil-steel flexible culvert: role of apparent cohesion of backfill

Maciej Sobótka and Dariusz Łydżba

Faculty of Civil Engineering, Wrocław University of Science and Technology, Wrocław, Poland

ABSTRACT

The article deals with the numerical modelling of a soil-steel structure subjected to live loads. The study refers to measurements obtained on a real culvert located near Niemcza village, Poland. The vehicle constituting the load was crossing the bridge one way and then it was going back. During such loading cycle the values of displacement and unit strain in chosen reference points on shell were registered. The graphs of measured quantities versus load location exhibit hysteresis loops. This feature of soil-steel structures is called hysteretic live load effect. The numerical simulation of the live load test was carried out using finite volume method. It was found that the hysteretic effect can be reproduced in the numerical model providing that Mohr-Coulomb model of soil backfill and one sided frictional interface at soil-steel contact were assumed. Furthermore, it has been shown that fair agreement of simulation and measurements results in both quantitative and qualitative aspect can be reached under the condition that the soil medium is treated as partially saturated by adopting adequate value of apparent cohesion.

ARTICLE HISTORY
Received 7 September 2018
Accepted 16 September 2019

KEYWORDS
Buried structure; hysteresis; vehicular loading

1. Introduction

Owing to their advantages, soil-steel structures are often used in practice today. Road and railway bridges and flyovers, and also wildlife crossings, tunnels, underground warehouses and linear municipal facilities (e.g. sewers) are built using this technology. This technology is also used to strengthen, repair and remodel the existing structures being in poor condition (e.g. Vaslestad, Madaj, Janusz, & Bednarek, 2004). The principal benefits resulting from the use of this technology are:

- relatively low construction costs,
- speed of construction,
- maintenance-free operation owing to the absence of bearings or expansion joint devices, and quite a long service lifespan of 50-60 years.

The peculiar character of flexible buried structures stems from the interaction between the backfill and the steel shell (e.g. Bayoglu Flener & Sundquist, 2007; Kunecki, 2006; Mellat, Andersson, Pettersson, & Karoumi, 2014; Seguini & Nedjar, 2017). Compliant shells, usually made

CONTACT Maciej Sobótka maciej.sobotka@pwr.edu.pl Faculty of Civil Engineering, Wrocław University of Science and Technology, Wybrzeże Wyspiańskiego 27, Wrocław 50-370, Poland

of corrugated steel plates, are characterized by very low stiffness and strength in comparison with those of typical structural members of conventional bridges. Therefore, concerning flexible soil-steel bridge structures, many authors suggest that the backfill soil should be treated as a structural element, e.g. (Machelski, Antoniszyn, & Michalski, 2006). Then, the soil medium transmits the load from vehicles to the shell and to the subsoil. This transmission depends on the interaction of the soil and the shell. Although the load-bearing capacity of each of the separate elements (shell and backfill) is too low, thanks to properly induced interaction between them, soil-steel structures can carry operational loads appropriate to their intended use. In that sense this interaction can be considered as synergistic advantageous effect. On the other hand, because of their peculiar character, deriving from the load bearing function of the backfill, the behaviour of soil-steel structures is qualitatively different from that of steel or reinforced concrete bridges. Civil structures with a compliant shell exhibit several nonlinear behaviour characteristics unique to them (e.g. Bayoglu Flener, 2010; Mai, Moore, & Hoult, 2014). This is a challenge for modelling which poses some difficulties. It is worth emphasizing that modelling states an important issue since it is indispensable element of the design process and at the same time is a valuable tool to describe phenomena from the theoretical point of view.

Due to its complexity the mechanical behaviour of buried structures is usually modelled with the aid of numerical methods such us finite element analysis (e.g. El-Sawy, 2003; Kunecki, 2014; Luo, Li, Tan, Ma, & Hu, 2018; Pettersson, Bayoglu Flener, & Sundquist, 2015) or finite difference method (Sobótka, 2014; Sobótka & Machelski, 2016; Tian, Liu, Jiang, & Yu, 2015) or coupled finite-discrete element method (Ahmed, Tran, & Meguid, 2015). Modelling contributes to better understanding of the structure behaviour by testing hypotheses (e.g. Sobótka, 2014) or analysing sensitivity to selected material and design parameters (Ahmed et al., 2015; El-Sawy, 2003; Yeau, Sezen, & Fox, 2014). In addition numerical modelling is extremely useful for the analyses considering random aspects of soil properties (Seguini & Nedjar, 2017; Tani, Nedjar, & Hamane, 2013) as well as for performing shape optimization of buried structures (Sobótka & Łydżba, 2014).

This article deals with numerical modelling of hysteretic live load effect. The latter is an interesting evidence of nonlinear behaviour of soil-steel structures. It was identified experimentally, independently in several soil-steel structures by in situ tests (Machelski et al., 2006; Machelski & Michalski, 2005). The effect lies in the fact that the structure's response to moving loads depends not only on the location and intensity of the load, but also on the direction of its movement. Aiming to investigate the nature of hysteretic live load effect several attempts were made so far to reconstruct it in a numerical model (Machelski & Marcinowski, 2007; Sobótka, 2014; Sobótka & Machelski, 2016). Although the hysteresis have been obtained (qualitatively), explicit explanation of the reasons for such behaviour remains an unsolved problem. Probably the effect of hysteresis is influenced by many factors. In the author's previous work (Sobótka, 2014) it was shown that the frictional nature of soil-shell contact zone is of particular importance. Nevertheless, it is reasonable to suppose the other factors such as non-linear elasticity, accumulated changes in the pore pressure, plastic hardening/softening of soil or effects of its partial saturation with water to play also an important role. From many analyses presented in the author's doctoral thesis (Sobótka, 2015) it follows that the effect of increased strength of soil due to partial saturation of its pores with water is particularly significant and clear. This work aims to show this effect. Thus, the simplest model capable of taking such increased strength into account is adopted for backfill soil, namely Mohr-Coulomb elastic-perfectly plastic with the, so called, apparent cohesion. In this manner, the other effects are omitted and the focus is on the role of the apparent cohesion.

The considerations refer to the results of numerical simulations of the test conducted originally by Machelski et al. (2006). Therefore the results of in situ measurements were the base for verification of model assumptions. In particular, the following hypothesis was put and positively verified: the peculiarities of the behaviour of the investigated structure can be both: qualitatively and quantitatively reproduced in the quite simple numerical model providing adoption of appropriate assumptions, in particular the proper value of apparent cohesion.

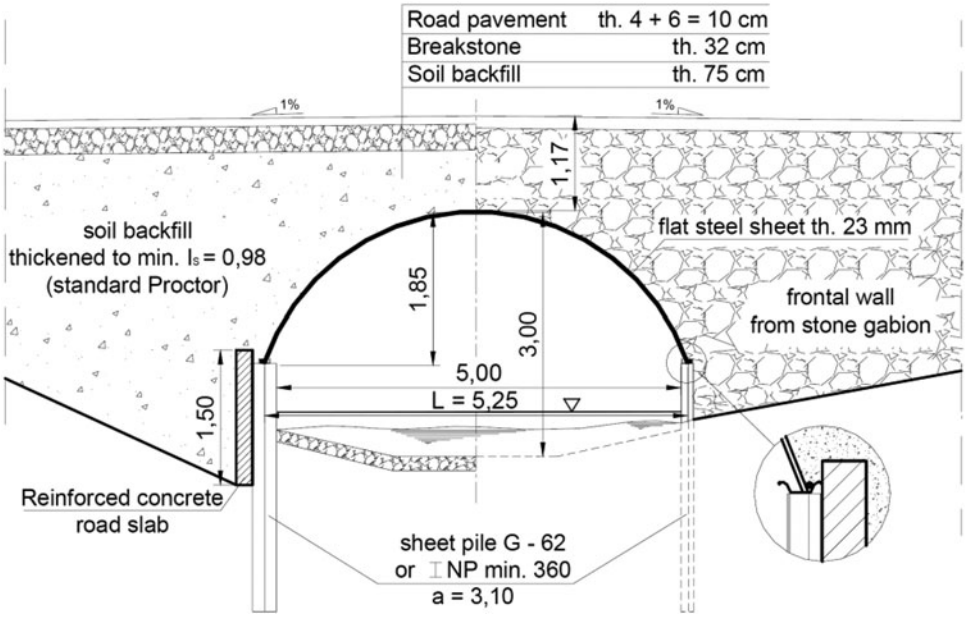

Figure 1. Longitudinal cross section of tested bridge.

2. Behavior of structure under live load: bridge in Niemcza

The bridge, being the object of test conducted by Machelski et al. (2006), is a single-span soil-steel structure with a span of about 5.0 m, built as a detour bridge carrying national road no. 8 near Niemcza, Poland. The shell, having the shape of a circular arch, was made of 23.0 mm thick flat steel sheet. Figure 1 shows the longitudinal cross section of the bridge.

2.1. Testing procedure

The tests carried out on the considered bridge consisted in measuring displacements and strains increments on the bottom surface of the shell under a moving load in the form of a dumper truck filled with soil. The loading scheme is shown in Figure 2.

During the test the truck would drive over the bridge first in reverse gear reversely to the sense of the *x*-axis (to the left) and then would return—drive in the opposite direction (to the right) without turning back. The drive proceeded in a quasi-static manner, which means that the vehicle drove slowly from one marker to the other and the measurements were taken while the truck was stopped. The forces transferred from the vehicle's particular axles to the bridge amounted to: $P_1 = 54.0$ kN (the front axle), $P_2 = 129.0$ kN (the middle axle), and $P_3 = 102.0$ kN (the rear axle).

In order to unequivocally specify the location of the truck (load) on the bridge, markers with consecutive numbers i were placed along the road at a spacing equal to half of the distance between the vehicle's second and third axle, i.e. at every 0.675 m, with the marker bearing the number $i = 0$, situated on the symmetry axis of the bridge (Figure 2). Readings were taken from the measuring instruments each time the vehicle's middle axle P_2 was situated in one of the marked consecutive points i. Thus the location of the vehicle along the road is described by the conventional coordinate i on which the vehicle's middle axle P_2 is situated.

2.2. Selected results

The results of tests carried out during two bridge construction stages, i.e. before and after deck paving, can be found in original research report (Machelski et al., 2006). Two loading plans, i.e.

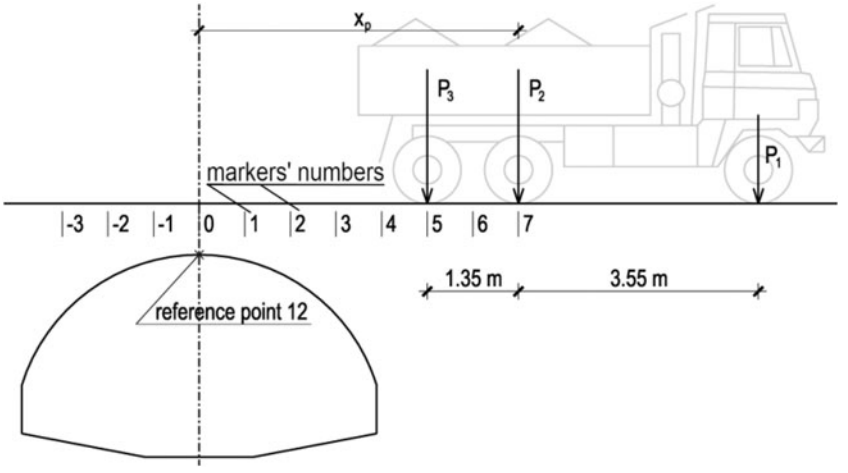

Figure 2. Test configuration.

driving along the road axis (central setting) and along the axis of one of the two lanes (lateral setting), were carried out in each of the two stages. In the present article references are made only to the test with the vehicle central setting, without the bridge deck pavement. A proper range of test vehicle movement, limited by the extreme positions: $i_{max} = 7$ and $i_{min} = -3$, was adopted to avoid a pronounced influence of load P_1 transferred from the first (the lightest) vehicle axle on the results.

A graph of the vertical displacement of the shell in its crown point (reference point no. 12 in the original research report; see Figure 2) and a graph of the stress on the bottom of the shell in the same point are presented in Figure 3(a,b), respectively. The vertical axis in the diagrams shows the measured quantities while the numbers of marker points i specifying the location of the load (axis P_2 to be more precise) are provided on the horizontal axis.

2.3. Comments on the results

The diagrams cited above (Machelski et al., 2006) clearly show hysteresis loops. The branches of the curves, corresponding to the successive ('there' and 'back') travels of the truck over the bridge, do not coincide—are drawn apart. The particular branches are shifted in the direction in which the load moves, i.e. the lines corresponding to the travel leftwards (the bold line) are shifted to the left while the branches corresponding to the travel rightwards are shifted to the right.

One should also note another interesting feature of the diagrams shown in Figure 3, connected with the differences in the values of the measured quantities (deflection/stress) in the particular ordinates. It is rather obvious that the maximum values in the diagrams correspond to the ordinates in which one of the axles is situated directly above the measuring point. Ordinate $i = 0$ corresponds to a vehicle location in which axle P_2 is situated above the measuring point, whereas ordinate value $i = 2$ means that axle P_3 is situated there. Local maxima appear near the ordinates, in both the displacement diagram and the stress diagram. It is easily apparent that the values (Figure 3) reached in ordinates $i = 0$ and $i = 2$ are different depending on the travel direction. This situation would not occur in an elastic structure. Then the measured deflection/stress values would depend on the values of forces P_1 and P_2 and on the load location (i.e. the value of ordinate i), but not on the travel direction. If the considered structure behaved elastically, the deflection/stress value in ordinate $i = 0$ would always be higher than in ordinate $i = 2$, since $P_2 > P_3$. But this dependence does not hold true for the considered structure. It is the

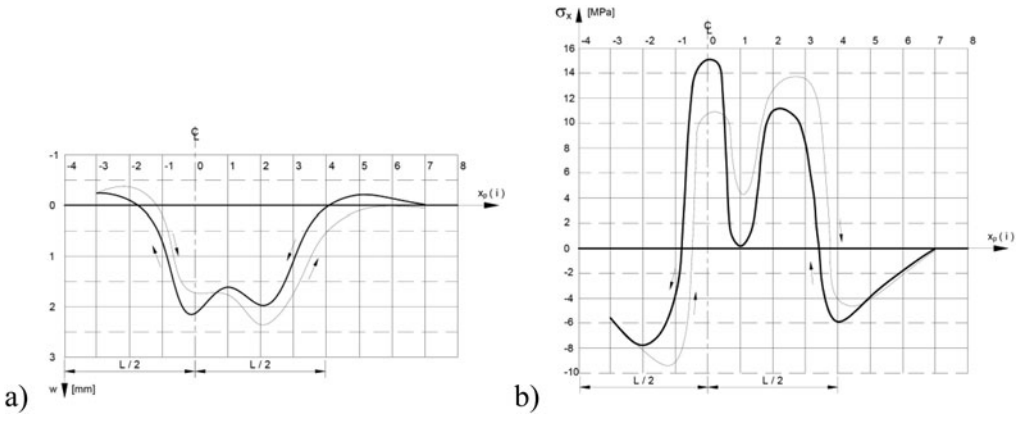

Figure 3. Diagrams showing results of measurements in reference point 12 (shell crown): a) vertical displacement, b) normal stresses on shell bottom.

travel direction which mainly determines in which of the ordinates ($i = 0$, $i = 2$) a higher value is registered. In particular, during the travel leftwards, first—when axle P_3 is situated over measuring point 12 (in location $i = 2$)—lower displacement and stress values occur and then—when axle P_2 appears over this point ($i = 0$)—higher values are observed. The reverse happens during the return, i.e. during the travel rightwards. Then first axle P_2 passes over point 12 and subsequently axle P_3. In this case, the measured values are higher in ordinate $i = 2$, i.e. under axle P_3, despite the fact that $P_3 < P_2$. In other words, if the vehicle moves one way, the effect of the forces successively appearing on the structure keeps growing (as reflected in the registered maximum displacement/stress values). However, it is worth noticing that a closed load cycle (there and back travel) generates practically closed hysteresis loops. In other words the displacement and stress take practically the same values before and after the loading cycle ("there" and "back" travel). It suggests that hysteresis loops would be repeatable if the structure was subjected to consecutive loading cycles.

3. Numerical model

The numerical model of the bridge was developed using Itasca Flac 7.0. The finite volume method grid with one-dimensional (beam and interface) elements is shown in Figure 4. The boundary conditions presented in Figure 4 are for the test start, i.e. truck location $i = 7$.

The computations were performed based on the procedure described in (Sobótka, 2014), but this time a more realistic constitutive backfill model, i.e. the elastic-plastic Mohr-Coulomb model with the non-associated plastic flow rule, was used. The backfill parameters were initially estimated on the basis of the local correlations included in the Polish standard for designing foundations PN 81/B 03020. The details of choosing proper backfill strength parameters and their discussion are provided in 3.2.

A linear-elastic model was adopted for the beam elements forming the shell and for the steel profiles in the piled wall. A one-sided contact was assumed at the steel shell-soil interface, which means that separation (pulling off) of the soil medium from the shell if the latter moves away from the backfill material and the subsequent "renewal" of the contact if the shell and the backfill come close together again are allowed. The shear stress value in the contact elements is limited by the Coulomb condition $|\tau_f| \leq a - \sigma \mathrm{tg}\delta$. Adhesion and soil-steel friction angle were assumed as in (Sobótka, 2014): $a = c = 0$ and $\delta = {}^2/_3 \cdot \phi$ where c and ϕ represent the backfill's cohesion and internal friction angle, estimated in accordance with the recommendations included in the polish standard PN 81/B 03020. The dilatancy angle for the contact elements was assumed

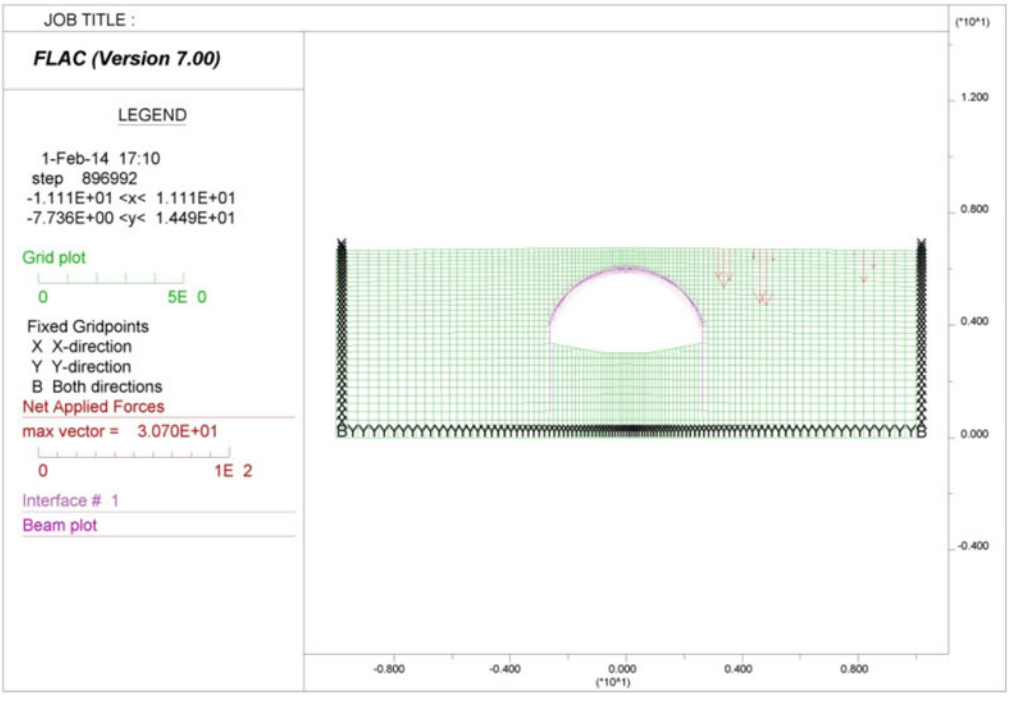

Figure 4. Numerical bridge model – finite volume grid and boundary conditions (for initial truck location $i = 7$).

as $\psi = 0$. The normal and shear stiffness parameters of an interface were calculated according to the software manufacturer recommendations included in the Flac 7.0 user's guide, which is described in more detail in (Sobótka, 2014).

3.1. Simulation procedure

In the first step of the computations the problem in which the only load was the dead load of the structure (the backfill, the shell and the foundation (pile wall)) was solved. Then the vehicle load in its initial location $i = 7$ was applied at the boundary (Figure 4). It was assumed that the load of each of the vehicle axles is transferred to the soil uniformly in a 0.5 m wide band (Figure 5). Considering that the load is distributed along the vehicle's width of 1.8 m (in the out of plane direction), the load values corresponding to axles P_1, P_2 and P_3 amount to $q_1 = 60.0$ kN/m, $q_2 = 143.3$ kN/m and $q_3 = 113.3$ kN/m. The calculation procedure requires that the loads must be converted to an equivalent system of forces in the nodes of the grid, as schematically shown in Figure 5. The grid of finite volumes is marked green, the band load – black and the vectors of the nodal forces are marked red.

The state of displacement and stress determined in the first step of the computations was used as the reference state corresponding to the test (measurement) start. The results presented further in this article take into account the fact that during the real in situ test (Machelski et al., 2006) increments relative to the initial reference state of displacement and stress (indirectly calculated from strain) were measured. In other words: before the test there had already been a certain nonzero state of displacement/stress in the structure, but the readings of the measuring devices were zeroed. Therefore in order to make a comparison of the test results and the simulation results possible the diagrams presented further in this article also refer to the increments relative to the reference state at the test start. In particular, the stress on the bottom surface of the shell, presented here as a simulation result and corresponding to the experimentally

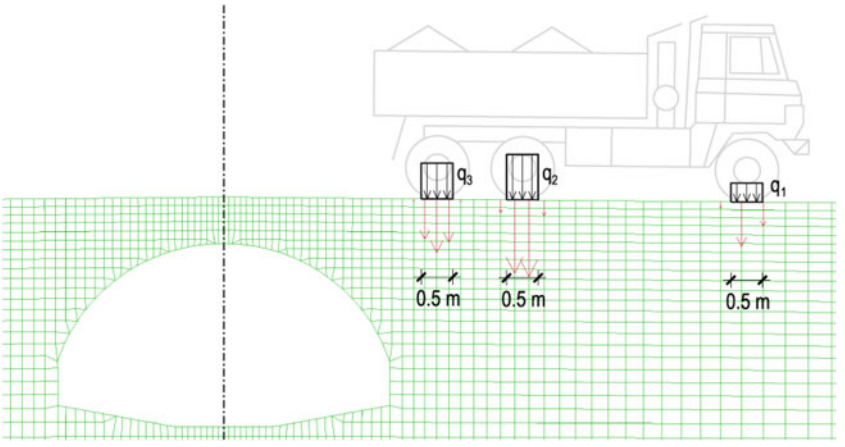

Figure 5. Scheme of vehicle load application.

measured stress (Machelski et al., 2006), was calculated, on the basis of the calculated internal forces, from

$$\sigma_x = \frac{(N-N_0)}{A} + \frac{(M-M_0)}{I} \cdot \frac{h}{2}, \tag{1}$$

where M, N stand for, respectively, the bending moment and the axial force, M_0 and N_0 are the moment and axial force values for the calculated state of the structure at the test start, h is the thickness of the steel shell, A and I are the cross-section area and moment of inertia, respectively.

The next simulation steps correspond to those of the moving load test (Machelski et al., 2006). The load was defined in the model step-by-step as a staged construction and static solution was found at each stage. This reflects the quasi-static character of the original test—the load would be moved a certain small distance and the problem would be solved after each shift. The distance between the successive locations amounted to 0.0675 m, i.e. 1/10 of the distance between the consecutive markers i in the original test. Consequently, a single travel between the locations $i_{max} = 7$ and $i_{min} = -3$ was effected through one hundred consecutive shifts. In comparison with the original test, not two, but six vehicle travels over the bridge, i.e. three full load cycles, with a full load cycle consisting of a 'there' travel and a 'back' travel, were assumed in the numerical analysis.

3.2. Mechanical parameters of backfill soil

The shell was backfilled with residual soil. Its dominant fraction was sand but it contained also the small amount of coarser (gravel and cobble) as well as finer (clay and silt) fractions. Since the data form laboratory tests is unavailable the mechanical parameters were initially estimated with the use of local correlations provided in (PN 81/B 03020). Compact coarse sand (compaction index $I_D = 0.8$) was assumed. The elasticity constants are the same as given in (Sobótka, 2014), i.e. $E = 150$ MPa, $\nu = 0.25$. In the present work the set of material constants was made complete by adding the values of the backfill's internal friction angle, dilatancy angle, and cohesion. The first of the parameters was assumed according to (PN 81/B 03020) as $\phi = 34.0^\circ$. In order to define the plastic flow rule, dilatancy angle ψ amounting to 10%·of internal friction angle ϕ, i.e. $\psi = 3.4^\circ$, was assumed for the computations. According to (PN 81/B 03020), cohesion should be assumed as $c = 0.0$ kPa.

When the elastic-perfectly plastic Coulomb-Mohr model of the backfill with its strength parameters determined according to standard PN 81/B 03020 was used, the obtained results

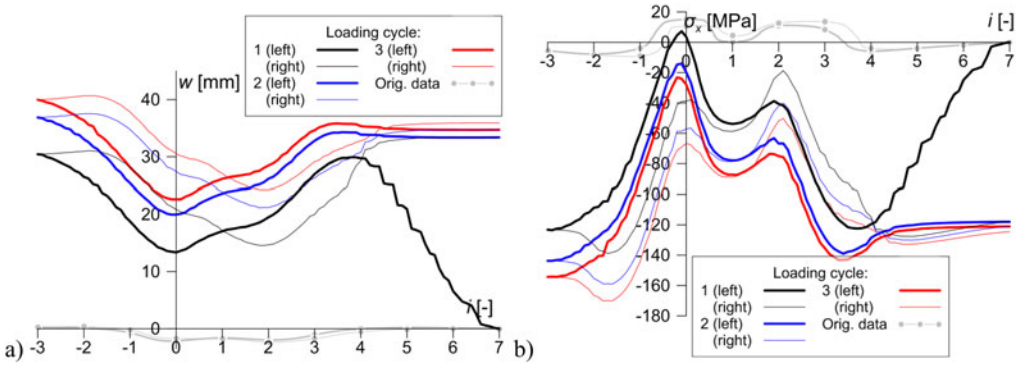

Figure 6. Vertical displacement (a) and stress on shell bottom (b) in reference point 12. $c = 1.0$ kPa.

differed considerably from the experimental ones (refer to Figure 6). Therefore it was necessary to check whether the adopted parameter values were correct. Standard PN 81/B 03020, complied with when calculating the soil parameters, provides that for given soil its mechanical parameters such us Young's modulus E and internal friction angle ϕ depend on state of compaction only. Then first, the efforts were made by the author to calibrate the model based on these parameters. The try, however, did not give satisfactory results. Changing these parameters even in a fairly wide range of values did not change the obtained results in the qualitative sense. Therefore an attempt was made to determine other factors (beside state of compaction) that could have an impact on soil mechanical parameters. Based on the author's knowledge (supported by literature review made) one of the reasonable approaches is accounting so called apparent cohesion (e.g. Monnet, Mahmutovic, Boutonnier, & Taïbi, 2019; Zheng, Shao, Guo, & Zhang, 2018) being an additional soil strength resulting from matrix suction in unsaturated soils. Thus, a hypothesis is advanced that the behaviour of the considered soil-steel structure can be significantly affected by the fact that the backfill as a partially saturated medium exhibits higher strength which can be regarded as apparent cohesion. This hypothesis will be tested further in this section. First, the way of estimating apparent cohesion on the basis of the dependences found in the literature on the subject is presented. Irrespective of this, an appropriate parametric analysis was carried out to test the effect of taking apparent cohesion into account in the calculations, assuming successively several different values of this parameter in the numerical simulations. Such a procedure can be also regarded as an analysis of model sensitivity to the assumed value of apparent cohesion.

3.2.1. Estimation of apparent cohesion Cψ

Partially saturated or unsaturated soils are characterized by enhanced strength stemming from matrix suction (Fredlund, Morgenstern, & Widger, 1978; Fredlund, Xing, Fredlund, & Barbour, 1996; Gan, Fredlund, & Rahardjo, 1988; Vanapalli, Fredlund, Pufahl, & Clifton, 1996). This extra strength is usually taken into account as apparent cohesion C_ψ. (Fredlund et al., 1978, 1996; Gan et al., 1988). Considering this fact, the assumption of zero (or close to zero) value of cohesion c is justified only for soils being in a saturation state other than 'partially saturated', which practically means completely dry or completely saturated soil. In the case of soil-steel structures such states should be ruled out. Thus taking apparent cohesion into account in the calculations is well-founded.

Matrix suction, also referred to as suction pressure or pressure deficit, is a difference between the atmospheric air pressure and the pressure of the water adhering to soil particles. For soils with the degree of saturation below $S_r < 0.85$, Peterson proposed the following modification of the Coulomb condition (Vanapalli et al., 1996)

$$|\tau_f| = c' - (\sigma + u_a)\mathrm{tg}\phi' + C_\psi, \tag{2}$$

where C_ψ is the apparent cohesion, c' and ϕ' are the effective strength parameters of the medium and u_a is the air pressure. Equation (3) is consistent with the Fredlund et al. concept (Fredlund et al., 1978) in which the critical shear stress is calculated from

$$|\tau_f| = c' - (\sigma + u_a)\tan\phi' + (u_a - u_w)\tan\phi^b, \tag{3}$$

where ϕ^b is a characteristic angle defining the increment in soil strength as the matrix suction is increased. For low matric suction the value of angle ϕ^b in formula (3) corresponds to the value of the internal friction angle (Gan et al., 1988). According to Fredlund (2000) the relation (3) with $\phi^b = \phi'$ is valid for sand within the matric suction ranging from 0 to nearly 100 kPa. It corresponds to apparent cohesion values from 0 to above 50 kPa. Taking these facts into account and comparing the terms on the right side of Equations (2) and (3) one gets the following expression for apparent cohesion

$$C_\psi = (u_a - u_w)\tan\phi'. \tag{4}$$

Furthermore, if air pressure is assumed as the reference pressure, i.e. $u_a = 0$, the expression for soil shear strength gets simplified. As a result, the Coulomb condition with apparent cohesion taken into account assumes the form

$$|\tau_f| = c' + C_\psi - \sigma\tan\phi, \tag{5}$$

which is equivalent to the Coulomb condition, provided $c = c' + C_\psi$ and $\phi = \phi'$ are assumed. Eventually, since $c' = 0$ in non-cohesive soils, the total value of cohesion to be used in calculation is $c = C_\psi$. Thus, the enhancement of soil shear strength in the unsaturated zone is accounted in a simplest possible way. The application of condition (5) corresponds in this context to undrained analysis, i.e. without the need to determine explicitly pore pressure distribution.

Matric suction can be estimated as the capillary rise above the stabilized groundwater level. In the case of the structure investigated here this approach is justified since the structure crosses a water course. Matric suction in such a case is equivalent to negative capillary pressure

$$u_w = -H\gamma_w, \tag{6}$$

where H is the rise above the water level and γ_w is the specific gravity of the water. Taking into account the earlier relations, the increase in strength due to matrix suction in the form of apparent cohesion can be estimated from

$$C_\psi = |u_w|\tan\phi = H\gamma_w\mathrm{tg}\phi. \tag{7}$$

For example, the difference in height between the shell's top part and the water level amounts to about $h = 2.5$ m (Figure 1). Then the absolute matrix suction value is

$$|u_a - u_w| = |-u_w| = \gamma_w|H| = 9.81 \cdot 2.5 = 24.5\ \ [\mathrm{kPa}], \tag{8}$$

while the apparent cohesion value calculated from formula (7) amounts to

$$C_\psi = |u_a - u_w|\tan\phi = 24.5\ \ \mathrm{tg}(34,0^\circ) = 16.5\ \ [\mathrm{kPa}]. \tag{9}$$

The calculated value of apparent cohesion (9) should be regarded as an estimate for selected height $H = 2.5$ m above the water level.

4. Simulation results

The problem of cyclic travels of the truck over the bridge was simulated in accordance with the computational procedure described in Section 3. First, the displacement and stress state under the deadweight was determined at the cohesion value $c = 1.0$ kPa. Then, to present explicitly the

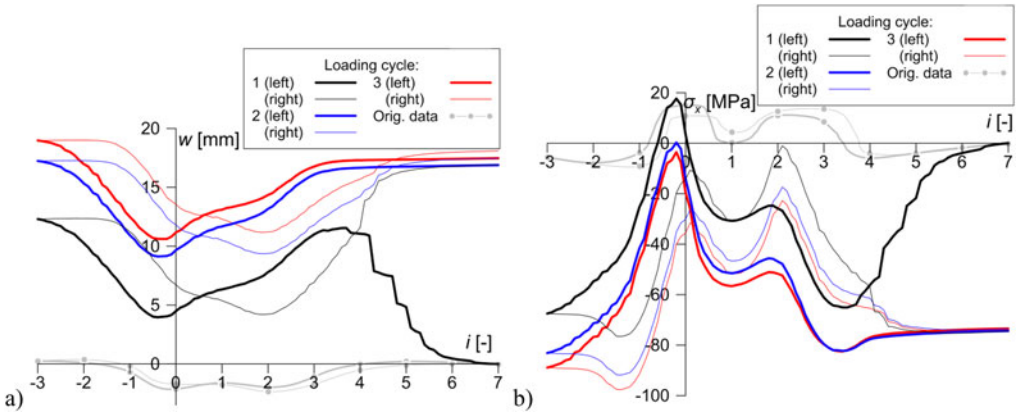

Figure 7. Vertical displacement (a) and stress on shell bottom (b) in reference point 12. $c = 5.0$ kPa.

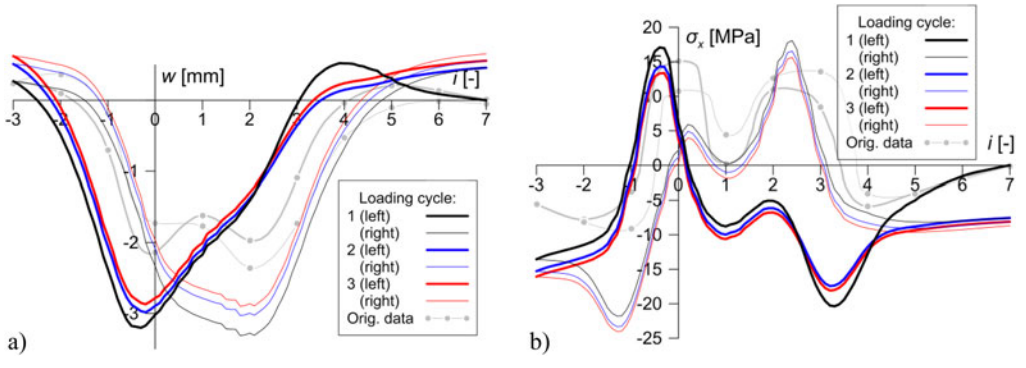

Figure 8. Vertical displacement (a) and stress on shell bottom (b) in reference point 12. $c = 10.0$ kPa.

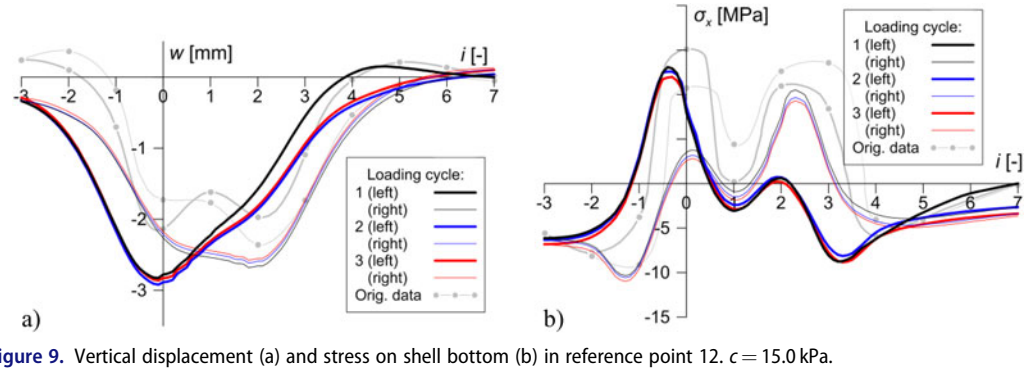

Figure 9. Vertical displacement (a) and stress on shell bottom (b) in reference point 12. $c = 15.0$ kPa.

effects of accounting apparent cohesion in simulation the parametric analysis was performed. The results of the simulation of the multiple vehicle travels over the bridge for the sequence of cohesion values c: $c = 1.0$ kPa, $c = 5.0$ kPa, $c = 10.0$ kPa, $c = 15.0$ kPa, $c = 20.0$ kPa, and $c = 50.0$ kPa are presented in Figures 6–11. The diagrams reflect directly the plots of displacement and stress in the shell bottom in reference point 12 as presented in Figure 3. The black lines represent the first load cycle, while the blue line and the red line correspond to the next load cycles, which were simulated. In order to make comparison with the measurement results (Machelski et al., 2006) the original data is also plotted in each graph. Similarly as in Figure 3, bold lines represent the first travel in a given load cycle (leftwards), while the fine lines represent the return travel

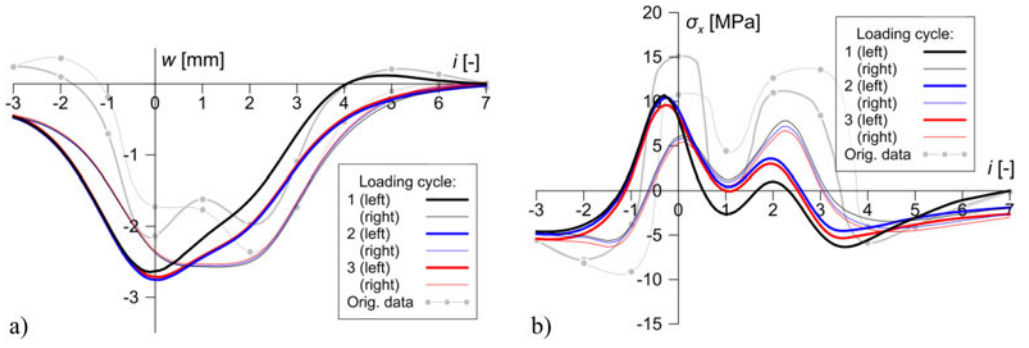

Figure 10. Vertical displacement (a) and stress on shell bottom (b) in reference point 12. $c = 20.0$ kPa.

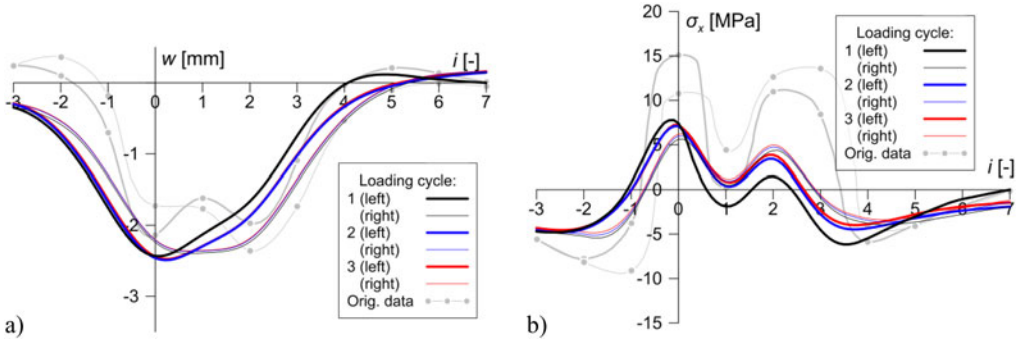

Figure 11. Vertical displacement (a) and stress on shell bottom (b) in reference point 12. $c = 50.0$ kPa.

(rightwards). Furthermore in Figure 12 the results for the first pass in the first loading cycle are summarized for all of the considered values of apparent cohesion.

5. Discussion

As can be seen in Figures 6–12, the simulation results are distinctly sensitive to the backfill cohesion value assumed in the calculations. Depending on the assumed apparent cohesion value, significantly different, both quantitatively and qualitatively, results are obtained.

If a too low value of parameter c (in a range of 1.0–5.0 kPa, Figures 6 and 7) is assumed, the obtained results considerably differ from the in situ measurement results (Machelski et al., 2006). A considerable uplift of the shell during the first travel of the vehicle and the gradual increment in the maximum uplift value in the successive load cycles are noticed. Similar qualitative observations apply to the stress diagram. In this case, the (absolute) values of circumferential stress σ_x are considerably overestimated in comparison with the measurements results (Machelski et al., 2006). Moreover, the (absolute) maximum values gradually increase in the consecutive load cycles (compare Figures 6 and 7 with Figure 3). In other words each subsequent vehicle pass induces permanent (irreversible) changes in the structure. Such results suggest that the overall soil strength (assumed in calculation) is too low to ensure required load bearing capacity of the structure under the assumed load. In contrast to the above, when cohesion values $c = 10.0$ kPa and higher (10.0, 15.0, 20.0, and 50.0 [kPa]) are adopted, almost closed hysteresis loops are obtained in both the displacement diagram and the stress diagram, which is qualitatively consistent with the in situ measurement results. This holds true starting from the second travel, while the first travel in the simulation (the black bold line in the diagrams) diverges from the trend.

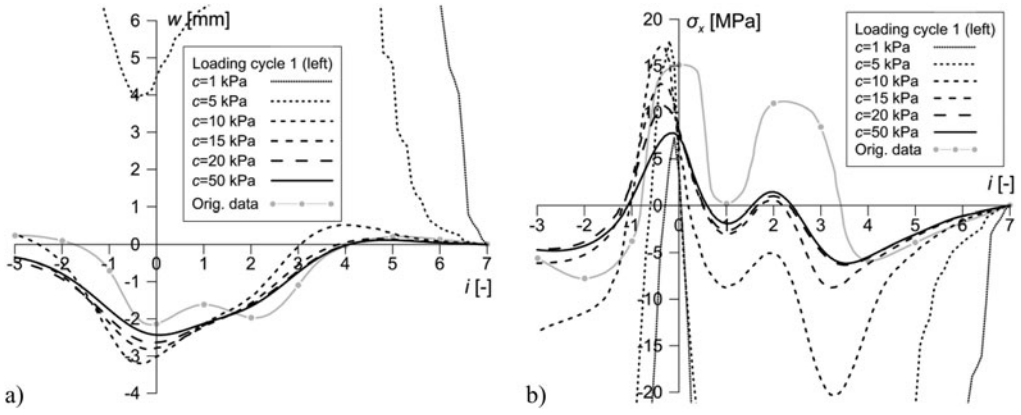

Figure 12. Vertical displacement (a) and stress on shell bottom (b) in reference point 12. Comparison of the results for different values of cohesion: first loading cycle (first travel, leftwards).

If a too high cohesion value ($c = 50$ kPa) is assumed, the simulation results do not indicate the effect (described in Section 2.3) manifesting itself in displacement and stress increment under the successive axles appearing on the structure. In this case (i.e. for $c = 50$ kPa) the values obtained in abscissae $i = 0$ and $i = 2$ are to a greater extent determined by the absolute values of forces P_2 and P_3 than by the effect mentioned above. In particular, in each of the six vehicle travels the displacement/stress value in abscissa $i = 0$ is always higher than in abscissa $i = 2$, regardless of the travel direction. Thus it can be concluded that if too high cohesion value is assumed then some of qualitative features of live load effect are not obtained in the model. In contrast to that, if cohesion values c lower than 50 kPa (i.e. 1.0, 5.0, 10.0, 15.0, and 20.0 [kPa]) are assumed, the simulation results qualitatively correspond to the measurement results. In particular, the travel direction determines in which of the abscissae ($i = 0$ or $i = 2$) the displacement/deflection value is higher. Thus the effect consisting in increment in the displacement/stress value registered under the successive vehicle axles has been reproduced in the numerical model.

As described above, the peculiarities of the behaviour of the real structure (described in Section 2.3) were successfully qualitatively reproduced in the simulations for the assumed apparent cohesion value of 10–20 kPa. Furthermore, the value of cohesion c for the investigated structure was determined in such a way that besides (qualitatively) reproducing the hysteretic effect, also quite good (quantitative) agreement between the simulation results and the measurement results was obtained. From among the analysed values the best results in comparison with the measurement results were obtained for $c = 15.0$ kPa (compare Figure 9 with Figure 3). Then the values of displacement w were within a range of –2.9 to 0.2 mm (as compared with the range of –2.5 to 0.5 mm in the real test), while the value of circumferential stress σ_x was in a range of –11.0 to 13.0 MPa (–10.0 to 15,0 MPa in the real test). It is worth noting that quite good quantitative agreement was obtained for both displacement and stress, without calibrating the other (apart from cohesion) model material parameters, for which the standard values given in the literature were adopted. Moreover, the 'calibrated' cohesion value $c = 15.0$ kPa, for which the best agreement between the simulation results and the experimental results was obtained, is closest (from among the values considered in the parametric analysis) to the one estimated according to the theoretical approach consistently with formula (9), i.e. $C_\psi \approx 16.5$ kPa.

In conclusion, it was presented that the effect of hysteresis in soil-steel structure can be reproduced (with accuracy sufficient for engineering applications) by means of relatively simple two-dimensional numerical simulations assuming elastic-perfectly plastic material of backfill soil. The interface in soil-shell contact zone allows sliding to occur. This feature was recognized by the author (Sobótka, 2014) to be significant from the point of view of modelling hysteretic live load effect. Furthermore, the present study takes the frictional nature of the backfill soil into account

by adopting Mohr-Coulomb model which is well-established in engineering practice. Certainly, the use of more advanced models should lead to result that was capable to reflect another feature of the behaviour of soil-steel structures. For instance, plastic hardening (of different types) has been considered in author's dissertation (Sobótka, 2015). It was presented that adopting such models led to obtaining the effects observed (in real structure) during multiply repeated load cycles.

In the article special attention was paid to a single parameter—the apparent cohesion. However, it must be noted that the other model parameters (those of elasticity and plasticity) must be properly selected. The above-mentioned doctoral thesis presented parametric analyses in which the sensitivity of the model was checked against friction angle in the interface, adhesion in the interface, Young's modulus of backfill and angle of internal friction of backfill. The analysis showed a significant sensitivity of the model to the values of the Young's modulus and the angle of internal friction of the backfill. However, the article focuses on cohesion since, in the authors' opinion, this parameter is particularly important for two reasons. First of all, there are clear physical reasons justifying the significant increase in strength, which stems from matrix suction due to partial saturation. This extra strength is usually taken into account as the apparent cohesion. In addition, a simple parametric analysis showed that the adoption of appropriate value of this parameter results in adequate compliance of simulation and in situ measurements—in both qualitative and quantitative sense. What is more, the cohesion value resulting in the best fit in the parametric analysis agrees with the value obtained from theoretical relations.

6. Summary and conclusions

The simulations of the behaviour of the soil-steel structure in Niemcza (Machelski et al., 2006) were carried out using the finite volume method and assuming a plain strain. Similarly as in (Sobótka, 2014), a one-sided frictional contact at the plate-soil interface was assumed in the numerical model of the structure, but the linear-elastic constitutive model of the backfill was replaced with an elastic-plastic model with the Mohr-Coulomb plasticity function. Moreover, the soil medium was treated as partially saturated by adopting apparent cohesion. Its value was first estimated using theoretical relations, but irrespective of this, a parametric analysis was carried out assuming several different values of apparent cohesion in the calculations.

The parametric analyses have shown that the behaviour of soil-steel structures is sensitive to the backfill soil cohesion value. It has been found that the peculiarities of the behaviour of the investigated structure can be qualitatively reproduced in the model if an apparent cohesion value of 10–20 kPa is assumed (with the other mechanical parameters estimated based on soil type using local correlations). Furthermore, for $c = 15.0$ kPa, besides qualitatively reproducing the hysteretic effect, also relatively good quantitative agreement was obtained for both displacement and stress. Moreover, the cohesion value $c = 15.0$ kPa resulting in the best fit in parametric analysis agrees with the value estimated using the theoretical relations, i.e. $c = C_{\psi} \approx 16.5$ kPa.

The presented results prove that the behaviour of soil-steel structures can be analysed accurately enough (for engineering purposes) by means of relatively simple 2D numerical models which can be created using commercial FEM of FVM (as in this article) computer programs. The key determinants of sufficient accuracy of such analyses are:

- the adoption of a frictional model of the soil-shell contact (interface) zone in the calculations and
- the adoption of an elastic-plastic constitutive model for soil medium and taking into account apparent cohesion. As presented in the article, the proper value of apparent cohesion is possible to estimate using simple theoretical relations.

Despite obtaining credible simulation results, the limitations of the approach used should be mentioned here. First, in the case of soil-steel flexible structures, 3D modelling would probably be more appropriate approach. However, from the point of view of everyday engineer's practice, the possibility of simplifying the problem to the 2D case is very useful. The analysis presented in the article proved such possibility. Nevertheless, in the scientific aspect, taking into account three-dimensional structure behaviour would certainly be very valuable. Such analyses will be for sure the topic of the author's future work. Secondly, while constructing or modelling soil-steel structures, the effect of staged backfilling is very important because it affects considerably the state of deformation and stress after the completion of construction. In the analyses presented in the article, the construction phases were not reproduced in the model. Nonetheless, not the absolute values of stress and displacement but their increments in relation to a reference state were considered. This was necessary to allow comparison with the results of the experiment (Machelski et al., 2006). Furthermore, the author tested different manners of accounting construction phases in the model. The results presented in the dissertation (Sobótka, 2015) follow to the conclusion that the way of taking construction stages into account has an impact on absolute values of stress and displacement but not on their increments.

In addition to the conclusions on numerical simulations, stated above, the following general conclusion follows from the considerations: the strength of the backfill, increased as a result of its incomplete saturation with water, has a significant effect on the behaviour of the investigated soil-steel structure subjected to live load. Thus, it emerges from this research that the proper behaviour of soil-steel structures is determined by the assurance of appropriate backfill moisture conditions. In particular, it is highly disadvantageous if the backfill is allowed to become fully saturated with water. Thus the suitable design of the backfill drainage system and maintaining the latter in good condition should be one of the priorities ensuring the safe and long-lasting operational use of soil-steel structures.

Disclosure statement

No potential conflict of interest was reported by the authors.

References

Ahmed, M. R., Tran, V. D. H., & Meguid, M. A. (2015). On the role of geogrid reinforcement in reducing earth pressure on buried pipes: Experimental and numerical investigations. *Soils and Foundations*, *55*(3), 588–599. doi:10.1016/j.sandf.2015.04.010

Bayoglu Flener, E. (2010). Testing the response of box-type soil-steel structures under static service loads. *Journal of Bridge Engineering*, *15*(1), 90–97. doi:10.1061/(ASCE)BE.1943-5592.0000041

Bayoglu Flener, E., & Sandquist, H. (2007). Field testing of a long-span arch corrugated-steel culvert under dynamic and static loads. *Archives of Institute of Civil Engineering*, *1*, 25–33.

El-Sawy, K. M. (2003). Three-dimensional modeling of soil-steel culverts under the effect of truckloads. *Thin-Walled Structures*, *41*(8), 747–768. doi:10.1016/S0263-8231(03)00022-3

Fredlund, D. G. (2000). The 1999 RM Hardy Lecture: The implementation of unsaturated soil mechanics into geotechnical engineering. *Canadian Geotechnical Journal*, *37*(5), 963–986. doi:10.1139/t00-026

Fredlund, D. G., Morgenstern, N. R., & Widger, R. A. (1978). The shear strength of unsaturated soils. *Canadian Geotechnical Journal*, *15*(3), 313–321. doi:10.1139/t78-029

Fredlund, D. G., Xing, A., Fredlund, M. D., & Barbour, S. L. (1996). The relationship of the unsaturated soil shear to the soil-water characteristic curve. *Canadian Geotechnical Journal*, *33*(3), 440–448. doi:10.1139/t96-065

Gan, J. K. M., Fredlund, D. G., & Rahardjo, H. (1988). Determination of the shear strength parameters of an unsaturated soil using the direct shear test. *Canadian Geotechnical Journal*, *25*(3), 500–510. doi:10.1139/t88-055

Kunecki, B. (2006). Full-scale test of corrugated steel culvert and FEM analysis with various static systems. *Studia Geotechnica et Mechanica*, *28*(2–4), 5–19.

Kunecki, B. (2014). Field test and three-dimensional numerical analysis of soil-steel tunnel during backfilling. *Transportation Research Record: Journal of the Transportation Research Board*, *2462*(1), 55–60. doi:10.3141/2462-07

Luo, Z., Li, Z., Tan, J., Ma, Q., & Hu, Y. (2018). Three-dimensional fluid–soil full coupling numerical simulation of ground settlement caused by shield tunnelling. *European Journal of Environmental and Civil Engineering*, 1–15. doi:10.1080/19648189.2018.1464961

Machelski, C., Antoniszyn, G., & Michalski, B. (2006). Live load effects on a soil-steel bridge founded on elastic supports. *Studia Geotechnica et Mechanica*, *28*(2–4), 65–82.

Machelski, C., & Marcinowski, J. (2007). Numerical modelling of moving load effect in a soil-steel bridge. *Archives of Institute of Civil Engineering*, *1*, 155–165.

Machelski, C., & Michalski, B. (2005). Odkształcenia mostowych konstrukcji gruntowo-powłokowych [Deformations of soil-steel bridges.]. *Drogi i Mosty*, *4*(2), 91–110.

Mai, V. T., Moore, I. D., & Hoult, N. A. (2014). Performance of two-dimensional analysis: Deteriorated metal culverts under surface live load. *Tunnelling and Underground Space Technology*, *42*, 152–160. doi:10.1016/j.tust.2014.02.015

Mellat, P., Andersson, A., Pettersson, L., & Karoumi, R. (2014). Dynamic behavior of a short span soil–steel composite bridge for high-speed railways–Field measurements and FE-analysis. *Engineering Structures*, *69*, 49–61. doi:10.1016/j.engstruct.2014.03.004

Monnet, J., Mahmutovic, D., Boutonnier, L., & Taïbi, S. (2019). A theoretical retention model for unsaturated uniform soils. *European Journal of Environmental and Civil Engineering*, *23*(3), 345–367. doi:10.1080/19648189.2016.1277376

Polska Norma, P. N. (1981). Grunty budowlane. Posadowienie bezpośrednie. Obliczenia statyczne i projektowanie [Building soils. Foundation bases. Static calculation and design]. PN 81/B 03020, Warszawa, Poland.

Pettersson, L., Bayoglu Flener, E., & Sundquist, H. (2015). Design of soil–steel composite bridges. *Structural Engineering International*, *25*(2), 159–172. doi:10.2749/101686614X14043795570499

Seguini, M., & Nedjar, D. (2017). Modelling of soil–structure interaction behaviour: Geometric nonlinearity of buried structures combined to spatial variability of soil. *European Journal of Environmental and Civil Engineering*, *21*(10), 1217–1236. doi:10.1080/19648189.2016.1153525

Sobótka, M. (2014). Numerical simulation of hysteretic live load effect in a soil-steel bridge. *Studia Geotechnica et Mechanica*, *36*(1), 104–109. doi:10.2478/sgem-2014-0012

Sobótka, M. (2015). Multiscale numerical modelling of the backfill-shell interaction in soil-steel structures. (In Polish) (Doctoral dissertation). Wrocław University of Science and Technology, Wrocław, Poland.

Sobótka, M., & Łydżba, D. (2014). Shape optimization of soil-steel structure by simulated annealing. *Procedia Engineering*, *91*, 304–309. doi:10.1016/j.proeng.2014.12.065

Sobótka, M., & Machelski, C. (2016). Hysteretic live load effect in soil-steel structure. *Engineering Transactions*, *64*(4), 493–499.

Tani, N. K., Nedjar, D., & Hamane, M. (2013). Non-linear analysis of the behaviour of buried structures in random media. *European Journal of Environmental and Civil Engineering*, *17*(9), 791–801. doi:10.1080/19648189.2013.822426

Tian, Y., Liu, H., Jiang, X., & Yu, R. (2015). Analysis of stress and deformation of a positive buried pipe using the improved Spangler model. *Soils and Foundations*, *55*(3), 485–492. doi:10.1016/j.sandf.2015.04.001

Vanapalli, S. K., Fredlund, D. G., Pufahl, D. E., & Clifton, A. W. (1996). Model for the prediction of shear strength with respect to soil suction. *Canadian Geotechnical Journal*, *33*(3), 379–392. doi:10.1139/t96-060

Vaslestad, J., Madaj, A., Janusz, L., & Bednarek, B. (2004). Field measurements of old brick culvert slip lined with corrugated steel culvert. *Transportation Research Record: Journal of the Transportation Research Board*, *1892*(1), 227–234. doi:10.3141/1892-24

Yeau, K. Y., Sezen, H., & Fox, P. J. (2015). Simulation of behavior of in-service metal culverts. *Journal of Pipeline Systems Engineering and Practice*, *5*(2), 1009–1016.

Zheng, G., Shao, L., Guo, X., & Zhang, J. (2018). Investigation of the mechanical behaviour of an unsaturated soil mixture using a digital image measurement system. *European Journal of Environmental and Civil Engineering*, 1–17. doi:10.1080/19648189.2018.1442258